ACS APPLIED MATERIALS & INTERFACES

www.acsami.org Forum Article

Cationic Molecular Umbrellas as Antibacterial Agents with Remarkable Cell-Type Selectivity

Ao Chen, Apostolos Karanastasis, Kaitlyn R. Casey, Matthew Necelis, Benjamin R. Carone, Gregory A. Caputo, and Edmund F. Palermo*

Cite This: https://dx.doi.org/10.1021/acsami.9b19076 Read Online

ACCESS | Metrics & More | Article Recommendations | Supporting Information

ABSTRACT: We synthesized a combinatorial library of dendrons that display a cluster of cationic charges juxtaposed with a hydrophobic alkyl chain, using the so-called "molecular umbrella" design approach. Systematically tuning the generation number and alkyl chain length enabled a detailed study of the structure−activity relationships in terms of both hydrophobic content and number of cationic charges. These discrete, unimolecular compounds display rapid and broad-spectrum bactericidal activity comparable to the activity of antibacterial peptides. Micellization was examined by pyrene emission and dynamic light scattering, which revealed that monomeric, individually solvated dendrons are present in aqueous media. The antibacterial mechanism of action is putatively driven by the membrane-disrupting nature of these cationic surfactants, which we confirmed by enzymatic assays on *E. coli* cells. The hemolytic activity of these dendritic macromolecules is sensitively dependent on the dendron generation and the alkyl chain length. Via structural optimization of these two key design features, we identified a leading candidate with potent broad-spectrum antibacterial activity (4−8 μg/mL) combined with outstanding hemocompatibility (up to 5000 μg/mL). This selected compound is >1000-fold more active against bacteria as compared to red blood cells, which represents one of the highest selectivity index values ever reported for a membrane-disrupting antibacterial agent. Thus, the leading candidate from this initial library screen holds great potential for future applications as a nontoxic, degradable disinfectant.

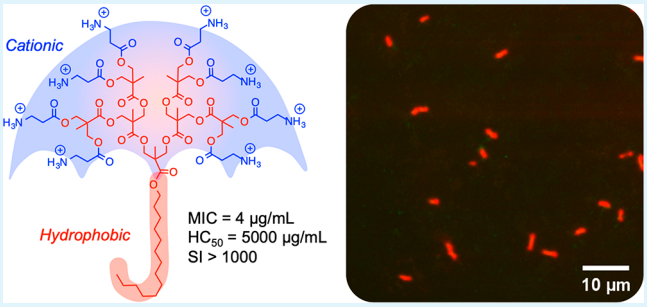

KEYWORDS: *antibacterial, dendrimer, hemolytic, cytotoxic, biocidal, biomembrane*

■ INTRODUCTION

Precise control of macromolecular structure has attracted increasingly focused attention in polymer chemistry and materials science.[1−6] In contrast to naturally occurring proteins that possess exquisite control of sequence, stereochemistry, and programmed secondary structures, conventional synthetic polymers are typically poorly defined, heterogeneous mixtures. Accordingly, near-perfect control of sequence, tacticity, dispersity, and chain branching have long been the most intensely sought-after visions in polymer chemistry, both historically[7,8] and at present.[9−12]

Host defense peptides (HDPs) act as components of the innate immune system in multicellular organisms.[13] These cationic and amphiphilic structures exert rapid and broad-spectrum antibacterial activity, either by direct membrane disruption and/or immunomodulary mechanism(s), without harming host cells and without readily inducing antibiotic resistance.[14,15] Synthetic oligomers and polymers have been widely shown to mimic the activity of HDPs by recapitulating the basic physiochemical features that are common to this class of peptides: cationic charge, amphiphilicity, and relatively short chain length.[16−19] Remarkably, even synthetic random copolymers with broad chain length dispersity and compositional dispersity are able to recapitulate the basic membrane-disrupting features of precisely structured HDPs.[20−24] Even still, strong arguments have been made in favor of precisely controlled macromolecular structures to precisely control antibacterial activity and toxicity.[25−28]

One of the most intensely discussed topics regarding rational design of HDP-mimetic antibacterial polymers is how best to spatially arrange the cationic and hydrophobic groups within the macromolecular architecture. HDPs tend to segregate their cationic residues and hydrophobic residues into distinct clustered regions of their secondary structures, often projected onto opposites "faces" of the structure.[29] This so-called "facially amphiphilic" design putatively facilitates localization at the lipid−water interface in anionic bacterial membranes.

Special Issue: Advances in Biocidal Materials and Interfaces

Received: October 22, 2019
Accepted: December 30, 2019

Molecular design strategies used to mimic such HDP structures include the so-called "same-center"[30−32] and "different-center" approaches,[33−35] as well as polymerization of facially amphiphilic monomer units[36] and side-chain functionalization of polymers with facially amphiphilic pendant groups (Scheme 1).[37] Each of these approaches has generated examples of formulations with potent antibacterial activity, and with varying levels of toxicity to human cells. In this work, we envisioned utilizing so-called "molecular umbrella"[38,39] amphiphiles, which display multivalent functionality on one face of a structure and pendant cargo centrally ensconced on the other. We hypothesized that such architectures could be exploited to facilitate bacterial membrane disruption. Specifically, we hypothesized that such structures might favor conformations in solution that conceal the hydrophobicity of the macromolecule beneath an array of cationic charges. Upon electrostatically driven binding to anionic bacterial membranes, the masked hydrophobic groups could then be inserted into the hydrophobic membrane core as a stealth payload. To that end, we targeted the design of cationic molecular umbrella amphiphiles that display dendritic multivalent cationic charge (as reversibly protonated primary amine groups) attached to a linear hydrophobic alkyl chain.

Scheme 1. Suite of Facially Amphiphilic (FA) Molecular Design Paradigms in Synthetic Mimics of HDPs Includes Same-Center, Different-Center, FA Backbone Units, and Pendant FA Units; In This Work, We Propose Molecular Umbrellas As a New Approach to Antibacterial Cationic Amphiphiles

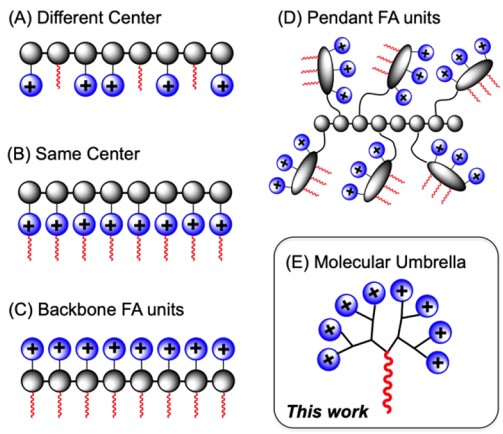

Dendrimers, and fragments thereof known as "dendrons", are hyperbranched macromolecules featuring a high density of functional groups per unit volume[40] (compared to linear polymers) and a high degree of structural precision/uniformity (compared to hyperbranched polymers). As such, dendrimers have been widely utilized in biomedical applications as multivalent carriers for host−guest complexing agents,[41] drugs,[42,43] and vaccines.[44,45] In cases where the functional groups on the dendrimer surface bear cationic charge, typically as quaternary ammonium salt (QAS) groups, these macromolecules are known to exert potent antibacterial activity at higher generations (G5 and above).[46−48] Prior examples also highlight the challenges associated with scalability and purity of antibacterial dendrimers, because the requirements of high generation number necessitate costly and laborious stepwise synthesis combined with difficulties in minimizing structural defects.[49] Recent examples have shown significant progress with grafting linear antibacterial polymers onto a lower-generation dendrimer core.[50,51] To best of our knowledge, only

Scheme 2. Synthesis of a Combinatorial Library of Cationic Molecular Umbrellas[a]

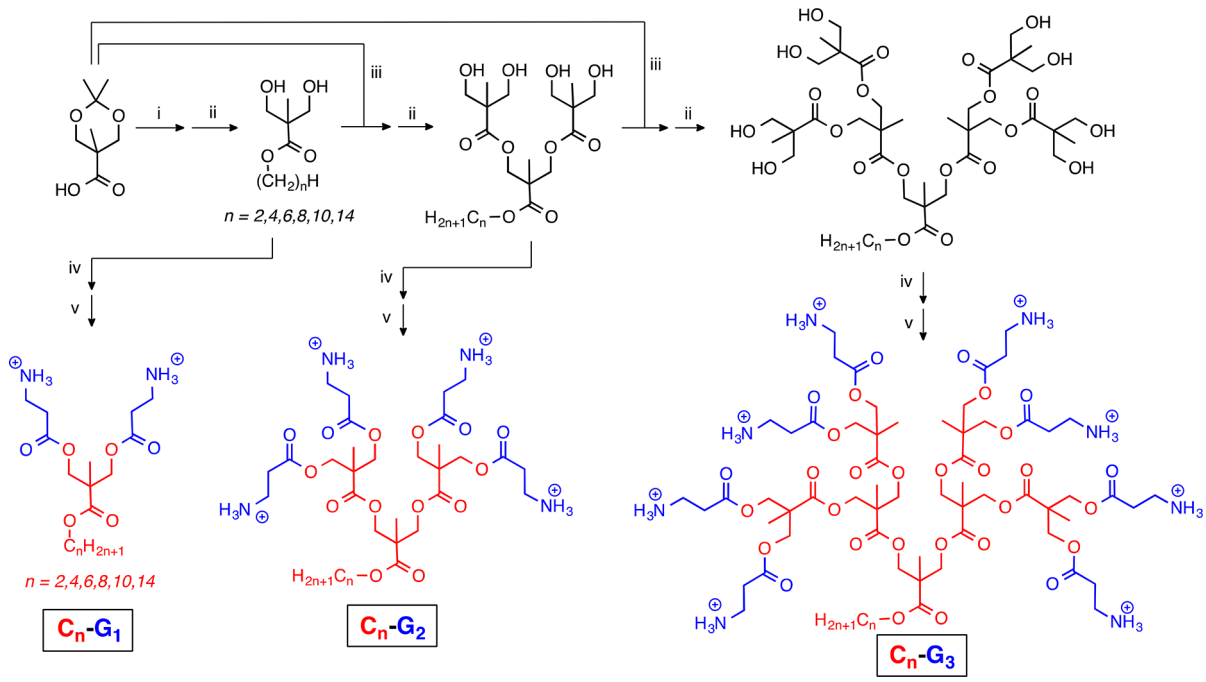

[a]Conditions: (i) (C_nH_{2n+1})−OH, DCC, DMAP, DCM, 0 °C; (ii) DOWEX-50W, MeOH, 50 °C; (iii) DCC, DMAP, DCM, 0 °C; (iv) Boc-β-alanine, DCC, DMAP, DCM, 0 °C; (v) TFA, neat, rt. TFA counter ions are omitted for clarity. All experimental procedures, purification procedures, and characterization data are given in detail in the Supporting Information.

https://dx.doi.org/10.1021/acsami.9b19076
ACS Appl. Mater. Interfaces XXXX, XXX, XXX−XXX

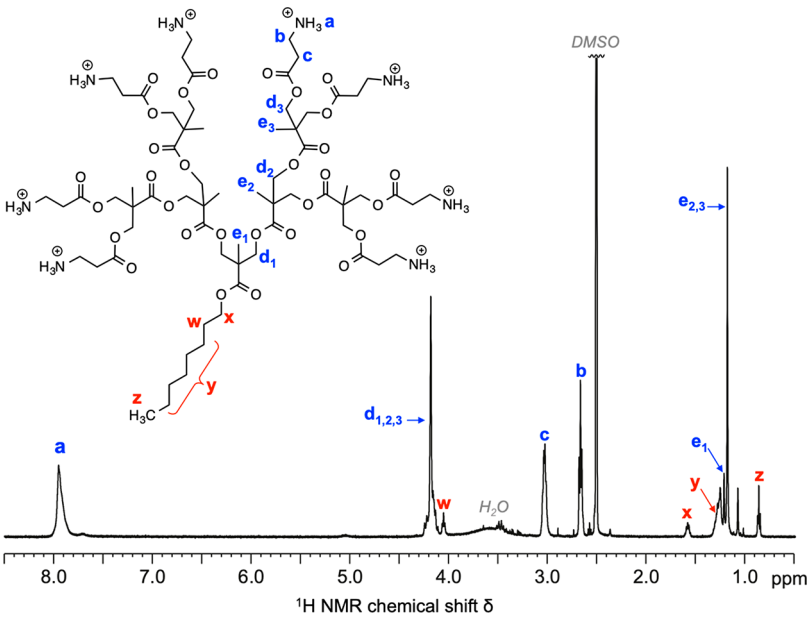

Figure 1. ^{1}H NMR spectra of $\mathbf{C_8G_3}$ in DMSO with peak assignments. Characterization of all intermediates and final compounds are given in the Supporting Information.

one prior study has explored facially amphiphilic antibacterial Janus dendrimers, which showed great promise.[52]

In this work, we sought to combine the concept of a molecular umbrella design platform and the advantages of precision dendron structures, with the goal of achieving potent antibacterial activity and high hemocompatibility at earlier generations (up to G3). We hypothesized that cationic dendrons directly bound to long hydrophobic alkyl chains would give rise to the desired combination of amphiphilic and multivalent structures. We chose to study dendrons composed of the unit 2,2′-bis(hydroxymethyl)propionic acid (bis-MPA) for reasons of synthetic accessibility and because of their structural resemblance to the widely studied antibacterial polymethacrylates.[24] We targeted protonated primary amines ($-NH_3^+$) as the source of cationic charge instead of the more commonly employed quaternary ammonium salts (e.g., $-N(CH_3)_3^+$), because the former have shown better cell-type selectivity in polymethacrylate systems.[35] Moreover, by systematically tuning the salient structural parameters (dendron generation number, alkyl chain length), we sought to precisely optimize the amphiphilic balance with the goal of enhancing efficacy at lower generation numbers than previously achieved with higher dendrimers. In this first exploratory library, with just 18 examples, we successfully identified a prime candidate for further study, which exhibits rapid and broad-spectrum antibacterial activity at low concentration (1−10 μg/mL) and is largely nonhemolytic even at very high concentrations (up to 5000 μg/mL). Thus, we report that a design platform focused on cationic molecular umbrella-like amphiphiles appears to be a good strategy to rapidly identify promising antibacterial agents.

■ RESULTS AND DISCUSSION

Dendron Synthesis and Characterization. We employed a divergent growth approach to build a combinatorial library of cationic dendrons with centrally attched alkyl tails, which we classify as "molecular umbrella" type amphiphiles. These compounds are designed to mimic the salient physiochemical features of host defense peptides and to bias the conformation of the macromolecules to encourage the formation of spatially segregated amphiphilic structures. Briefly, dendrons were synthesized by the repetitive condensation of a difunctional alcohol with acetonide-protected (2,2-bis(hydroxymethyl)propionic acid (bis-MPA), followed by deprotection of the acetonide group, according to precedent.[53] After building these polyesters to the desired dendron generation, we converted the alcohol functional groups of the dendron surface into primary amines by coupling to Boc-protected β-alanine, followed by TFA deprotection, which ultimately yielded the desired polycationic target structures (Scheme 2). In all steps, yields were consistently good to excellent. All intermediates and target compounds exhibited ^{13}C and ^{1}H NMR spectra in accordance with the proposed structures. Final product identity and purity was also confirmed by MALDI, which showed a single peak at the expected m/z (page S-94 in the Supporting Information).

Nomenclature. Our targeted library encompasses bis-MPA dendrons of the first, second, and third generations (displaying two, four, and eight cationic ammonium surface groups, respectively), each with one of six different pendant alkyl chains (ranging from C_2H_5 to $C_{14}H_{29}$) for a total of 18 compounds. The nomenclature used in this report is C_nG_x, where n refers to the alkyl chain length and x to the dendron generation. For example, the third-generation dendron with an octyl chain is named C_8G_3. An example ^{1}H NMR spectrum for C_8G_3 is shown (Figure 1).

Potentiometic Titration. Because these dendrons contain primary amines that are cationic by virtue of reversible protonation, it is necessary to delineate the pH range over which they remain largely or entirely protonated.[35] The extent of ionization for dendrons from each generation in aqueous media was assessed by potentiometric titration with 1N NaOH in 150 mM saline solution under a nitrogen blanket. Whereas the pK_a of the amine group in the small molecule β-alanine is about 10.3, the dendrons in this work containing β-alanine surface functionality have a pK_a that is somewhat suppressed

https://dx.doi.org/10.1021/acsami.9b19076
ACS Appl. Mater. Interfaces XXXX, XXX, XXX−XXX

due to Columbic repulsion between proximal cationic charges. For each dendron generation in this work, the pK_a values are in the range of 9.1−9.2. Thus, at the pH of the assay conditions described below (pH 7.4) approximately 98% of the amine groups should be present in the protonated ammonium salt form. It is well-known in the literature that cationic bis-MPA dendrimers chemically degrade in aqueous solution in a temperature- and pH-dependent manner.[54,55] Thus, we conducted further control experiments to verify that these compounds are stable in the storage conditions and the assay conditions tested here. We found that storage of the dendrons at 4 °C in an aq. stock solution of pH 4 for 2 weeks led to no discernible changes in the structure of the dendrons by NMR (see page S-100 in the Supporting Information). Also, no chemical change was noted by NMR when the dendrimers are incubated at 37 °C for 1 h at pH 7 (see page S-101 in the Supporting Information), which reflects the assay conditions used to test antibacterial and hemolytic activity (vide infra).

Micellization. It has been previously shown that supramolecular self-assembly is an important consideration in membrane-disrupting antibacterial agents.[56] Because the dendrons in this work are amphiphilic, one expects them to micellize in aqueous media above some critical micelle concentration (CMC). We examined the aggregation of these amphiphilic dendrons by a pyrene eximer emission assay (Figure 2A). In this method, serial dilutions of each

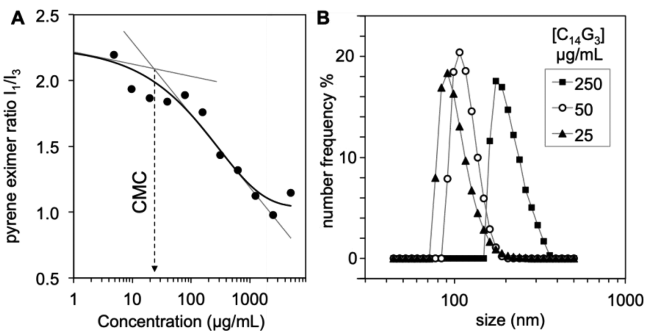

Figure 2. (A) pyrene fluoroesence assay with $C_{14}G_3$ to estimate critical micelle concentration (CMC) (B) size distribution of $C_{14}G_3$ micelles in PBS by dynamic light scattering (DLS). Combined, these data indicate a CMC of ∼23 μg/mL.

dendron were dissolved in pyrene-saturated PBS and equilibrated overnight at room temperature on a 96-well microplate. Fluorescence emission was then recorded at λ = 373 (I_1) and 384 nm (I_3) with excitation at λ = 334 nm for each well. The ratio of emission intensities (I_1/I_3) is commonly used to detect the chemical microenvironment of pyrene.[57] In aqueous solution, the ratio is about 2.3, whereas in hexanes, it is about 0.8. When mixed with amphiphilic dendrons in aqueous media, we expect that pyrene will partition into the hydrophobic core of any micelles that form above the CMC. Thus, observation of a trend in I_1/I_3 values approaching the value of 0.8 is strong evidence of self-assembled structures that possess a nonpolar core. To estimate the CMC, we first performed curve-fitting with a sigmoidal function and then took the intersection of the two tangent lines at the limit of low concentration and at the inflection point. By this method, the pyrene assay gives a CMC of 23 μg/mL for $C_{14}G_3$. Indeed, the molecular umbrella type dendrons appear to assemble into such micellar structures at high concentrations, provided that the alkyl chain tail is sufficiently long. For example, in the G1 series (contains a + 2 cationic charge), the dendron with the shortest alkyl chain, C_2G_1, did not show any evidence of pyrene partitioning up to the highest concentration tested (5 mg/mL). As the alkyl chain was elongated to butyl and hexyl, the G1-series dendrons showed weak evidence of micellization beginning around 5 mg/mL. For longer alkyl chains (C_8−C_{14}), G1 dendrons exhibit a typical sigmoidal dose−response curve with a characteristic CMC, which decreases with increasing alkyl chain length, as expected. For the G2 series, no evidence of micellization is observed for C_2−C_6 chains, and only weak evidence is seen for C_8 at 5 mg/mL. The more hydrophobic examples showed micellization at about 1 mg/mL for $C_{10}G_2$ and 20 μg/mL for $C_{14}G_2$. Finally, in the third generation (G3) series, only the example with the longest alkyl tail ($C_{14}G_3$) showed any evidence of stable aggregates based on pyrene emission (Figure 2A). G3 dendrons with all shorter alkyl chains showed no distinct sigmoidal curve, suggesting that pyrene was not portioning into a nonpolar environment, and thus no stable micelles existed.

Dynamic light scattering (DLS) was used to examine the size distribution of the aggregates formed in aqueous buffer by $C_{14}G_3$ (Figure 2B). Scattering intensity as a function of time was strong and erratic for solutions of $C_{14}G_3$ in PBS at concentrations ranging from 250 to 25 μg/mL, which generate autocorrelation functions $g^2(t)$ of high quality and good reproducibility (see the Supporting Information). Below 25 μg/mL, the intensity trace and $g^2(t)$ were both weak, which suggests that stable micelles are not formed. This cutoff agrees very well with the CMC by pyrene emission, 23 μg/mL. The dendron $C_{14}G_3$ showed micelles with a number-average particle size of 241 ± 50 nm at 250 μg/mL. When diluted to 50 and 25 μg/mL, the particle size decreases monotonically to 107 ± 18 and 91 ± 6 nm, respectively. Below the characteristic aggregation concentration found in the pyrene emission assay (e.g., at 12.5 μg/mL or lower), light scattering was weak and the size distributions were not reproducible, suggesting that the compounds are individually solvated in water under these dilute conditions. Importantly, the antibacterial activity of $C_{14}G_3$ is observed in the concentration range of 1−10 μg/mL range (vide infra). This finding suggests that the species is unimolecularly solvated in aqueous solution at the biologically active concentration. Further, one may interpret this result to mean that the unimolecular compound (not a micelle thereof) is the biologically active species. However, it is also possible that dendrons may assemble into aggregated structures upon binding to the biomembrane interface, as observed previously for AMPs.[58]

Antibacterial Activity. Each of the cationic molecular umbrellas in the library was initially screened for inhibitory activity against *E. coli* and *S. aureus* in nutrient-rich growth media by a turbidity-based, high-throughput assay in 96-well microplate format. The minimum inhibitory concentration (MIC) is defined as the lowest concentration of dendron in solution that completely prevents the growth of bacteria in standard incubation conditions (5×10^5 CFU/mL, MH broth, 37 °C, 18 h). Whereas the MIC reflects the inhibition of bacterial cell growth, it does not directly prove that bacteria are irreversibly inactivated (i.e., "killed"). Thus, we also tested the minimal bactericidal concentration (MBC). In all cases, the MBC is equal to MIC or 2 × MIC, which demonstrates that the dendrons are in fact bactericidal and not merely bacteriostatic (see the Supporting Information).

https://dx.doi.org/10.1021/acsami.9b19076
ACS Appl. Mater. Interfaces XXXX, XXX, XXX−XXX

Table 1. Antibacterial and Hemolytic Activities of Cationic Molecular Umbrellas

compd.	gen.	C_n	MW (g/mol)	MIC (μg/mL)		HC_{50} (μg/mL)	HC_{50}/MIC	
				E. coli	*S. aureus*	sheep RBC	*E. coli*	*S. aureus*
C_2G_1	G1	2	532	>1000	>1000	>5000		
C_4G_1		4	560	>1000	>1000	>5000		
C_6G_1		6	589	>1000	>1000	>5000		
C_8G_1		8	617	250	500	1514	6.1	3.0
$C_{10}G_1$		10	645	31.25	31.25	79.6	2.5	2.5
$C_{14}G_1$		14	700	3.9	3.9	10.1	2.6	2.6
C_2G_2	G2	2	1135	>1000	>1000	>5000		
C_4G_2		4	1163	>1000	>1000	>5000		
C_6G_2		6	1191	>1000	>1000	>5000		
C_8G_2		8	1219	>1000	250	>5000		>20
$C_{10}G_2$		10	1247	62.5	31.25	2500	40	80
$C_{14}G_2$		14	1303	3.9	1.95	63	16.1	32.2
C_2G_3	G3	2	2340	>1000	>1000	>5000		
C_4G_3		4	2368	>1000	>1000	>5000		
C_6G_3		6	2396	500	>1000	>5000	>10	-
C_8G_3		8	2424	125	62.5	>5000	>40	80
$C_{10}G_3$		10	2452	31.25	7.8	>5000	>160	>640
$C_{14}G_3$		14	2508	7.8	3.9	~ 5000	~ 640	~ 1280

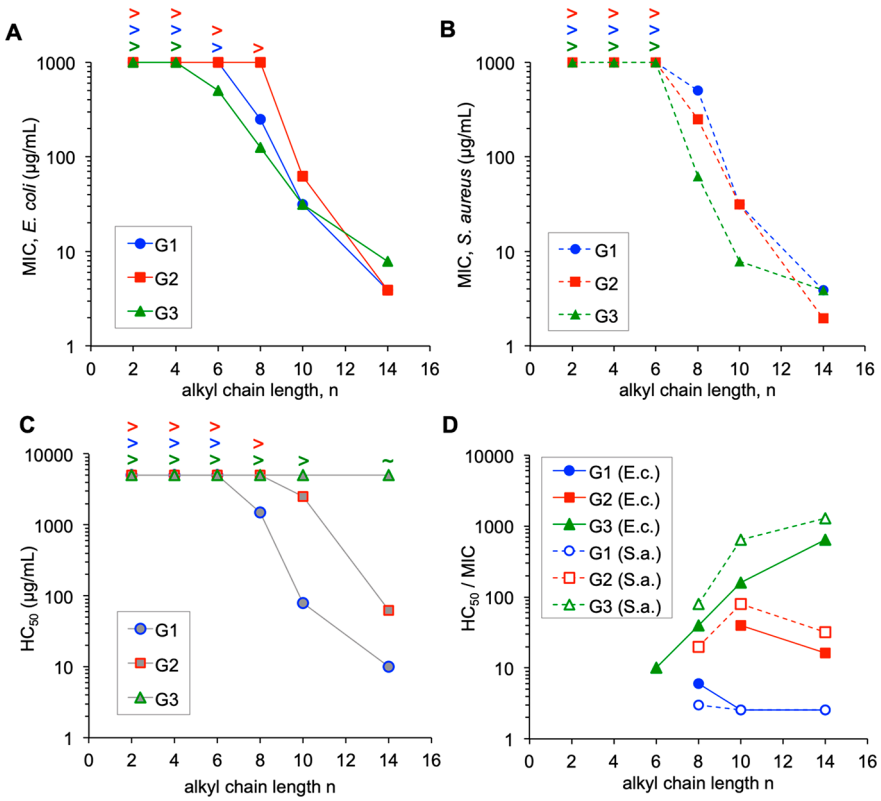

Figure 3. Semilog plots of MIC against (A) *E. coli* and (B) *S. aureus*, (C) HC_{50} against red blood cells, and (D) the selectivity index, HC_{50}/MIC as a function of alkyl chain length in each dendron generation. The ">" symbols indicate that the assay gave an activity that is greater than the data points as shown.

The antibacterial activity of these dendrons is strongly dependent the length of the pendant alkyl chain (hydrophobicity), as expected from the literature,[34,35,59] whereas the dependence on generation (number of cationic charges) is far less pronounced (Table 1, Figure 3A, B). In general, as the hydrophobicity increases, the antibacterial activity of the dendrons monotonically increases against both representative Gram−negative and Gram−positive bacterial strains. In the G1 series, the dendrons bearing C_2, C_4, and C_6 tails were inactive (MIC > 1 mg/mL); C_8G_1 was weakly active (250 μg/mL); $C_{10}G_1$ was moderately active (31 μg/mL) and only the most hydrophobic member of the series, $C_{14}G_1$, showed potent activity (4 μg/mL). Similarly, for the G2 and G3 series, shorter alkyl chains of C_2−C_6 failed to confer sufficient hydrophobicity and thus gave inactive or only weakly active dendrons. In contrast, the G2 and G3 dendrons with the longest alkyl chains

https://dx.doi.org/10.1021/acsami.9b19076
ACS Appl. Mater. Interfaces XXXX, XXX, XXX−XXX

(C_{14}) also gave potent antibacterial activity comparable to $C_{14}G_1$. Although the antibacterial activities of these dendrons did not appear to depend very sensitively on generation number, the hemolytic activities were extremely sensitive to the dendron generation (Table 1, Figure 3C).

Hemolysis. The membrane-disrupting toxicity to mammalian cells was assessed by a standard hemolysis assay using a suspension of sheep red blood cells (1% v/v, PBS, pH 7.4). As a positive control, the surfactant Triton-X 100 was used to fully lyse the RBCs. As a negative control, PBS alone with no compound was used to detect any background hemoglobin leakage. In accordance with prior work[35,59] on a broad range of antibacterial polymers, the most pronounced effects is an increase in hemolytic toxicity as a function of increasing hydrophobic character, across all samples in all three generations of dendron. Unlike the antibacterial activity, the hemolysis is sensitively dependent on dendrimer generation. For the dendrons with C_{10} alkyl tails, we find that the G1 compound is the most hemolytic (HC_{50} = 80 μg/mL), G2 is weakly hemolytic (HC_{50} = 2500 μg/mL), and G3 is totally nonhemolytic (HC_{50} > 5000 μg/mL). Thus, we find that the number of cationic charges has a profound effect on the hemolysis at a fixed length of hydrophobic alkyl chain. Since the hemolysis is widely understood to depend mostly on the overall hydrophobicity of the compounds, the simplest interpretation of these results is that higher generations have lower overall global hydrophobicity relative to the lower generations, even at a fixed alkyl chain length.

Remarkably, the hemolytic activity of the third generation G3-series of dendrons was extremely weak. These G3 dendrons bearing a wide range of alkyl tail chains (from C_2 to C_{10}) induced almost no hemolysis relative to background even up to the highest concentration tested (5000 μg/mL) and thus HC_{50} could not be determined. Only the G3 dendron with the longest alkyl chain, $C_{14}G_3$, showed any evidence of hemolysis, with about ~50% hemoglobin release at 5000 μg/mL. It was not possible to extract an exact value for the HC_{50} of this dendron, since curve-fitting is unreliable for the incomplete dose−response curve. Qualitatively, one may reasonably estimate that the HC50 of $C_{14}G_3$ is approximately equal to 5000 μg/mL. Since this dendron is a potent antibacterial agent (MIC = 7.8 and 3.9 μg/mL against *E. coli* and *S. aureus*, respectively), the lack of hemolytic toxicity implies exceptionally high cell-type selectivity for the putatively membrane-disrupting activity. We hypothesized that the precision molecular umbrella design of these antibacterial agents would endow them with a high propensity for localization at bacterial membranes, along with a high degree of cell-type selectivity. The selectively is often expressed as a ratio, HC_{50}/MIC. The best example in this small, targeted library of just 18 compounds gave HC_{50}/MIC ~ 1280, which is one of the highest such values ever reported, to the best of our knowledge. Thus, we find that the cationic molecular umbrella approach is indeed a fruitful design paradigm for rapid identification of optimally HDP-mimetic compounds.

Whereas the data in Table 1 and Figure 3 present activity in mass-dosage units (μg/mL), it is often also instructive to convert these data into μM units, the latter of which reflect the activity of individual molecules. Because the MW of the compounds in our library varies over a range of about 500 to 2500 g/mol, differences in activity expressed as μg/mL versus μM may be nontrivial. Nonetheless, plotting the data in molar units does not appear to substantially influence the overarching conclusions from this work: even when normalized to activity per mole, the dendrons show stronger antibacterial activity as a function of increasing alkyl chain length and are relatively less sensitive to generation number (see page S-88 in the Supporting Information). It is especially noteworthy to emphasize that the selectivity index HC_{50}/MIC is by definition unaffected by the choice of units. Because the most important outcome of this initial screening effort was the identification of a compound with especially high selectivity index, the choice of units is considered immaterial.

Bactericidal Kinetics. We also investigated the rate of bactericidal action against *E. coli* for the leading candidate compound from our initial screen, the third generation dendron with a 14-carbon alkyl tail, $C_{14}G_3$ (Figure 4A). We incubated *E. coli* cultures (3×10^5 CFU/mL) in nutrient-rich Muller-Hinton (MH) broth at 37 °C for 2 h, in the presence and absence of $C_{14}G_3$ at a concentration of 2 × MIC (16 μg/mL). The positive control sample, *E. coli* alone in MH, showed the expected growth curve as a function of time, ultimately reaching 3×10^6 CFU/mL after 2 h. In stark contrast, the number of viable *E. coli* cells in suspension decreases immediately and precipitously in the presence of $C_{14}G_3$. Within the first 30 min, the viable *E. coli* concentration undergoes about a 2-log reduction (99.7% killing). After 1 and 2 h incubation, 3.8 and 4.5-log reductions (99.9985 and 99.9997% killing) were observed, respectively. Thus, we conclude that this dendron is rapidly bactericidal under these solution-based conditions. Importantly, it appears that the rate of bactericidal action is more rapid than the rate at which these polyester bis-MPA type dendrons typically degrade by hydrolysis (37 °C, pH 7).[54,55] Therefore, it is reasonable to envision applications in which some formulation of the dendrons disinfects materials rapidly and then degrades to nontoxic byproducts on a slower time scale.

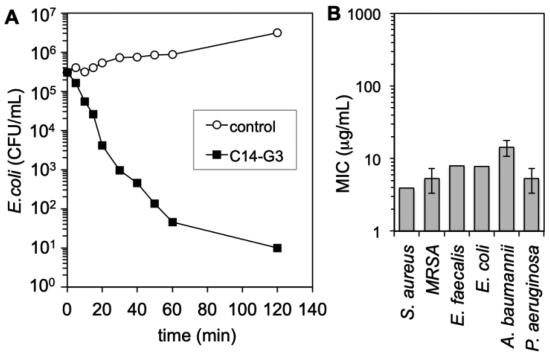

Figure 4. (A) Bactericidal kinetics and (B) activity against a broad-spectrum of Gram-positive and -negative strains.

Broad Spectrum. Our initial screening tested activity against just two representative microoganisms, Gram-negative *E. coli* and Gram-positive *S. aureus*. Upon identification of the leading candidate, $C_{14}G_3$, this compound was selected for more detailed testing against a broader panel of bacterial strains (Figure 4B). In general, it would appear that $C_{14}G_3$ shows no particular Gram-selectivity and is rather a potent broad-spectrum antibacterial agent with the ability to inactivate notoriously pathogenic microorganisms implicated in infectious diseases, including methicillin-resistant *S. aureus* (MRSA) and *A. baumannii*.

https://dx.doi.org/10.1021/acsami.9b19076
ACS Appl. Mater. Interfaces XXXX, XXX, XXX−XXX

Cytotoxicity. Activity against HeLa cells was assessed by monitoring metabolic activity (using a CellTiter Blue assay kit) in Dulbecco's modified Eagle's medium (DMEM) following 24 h incubation at 37 °C in vitro (Figure 5). We selected HeLa cells, which are cancerous and replicate more rapidly than primary cells, because they are a standard cell line widely used in the drug delivery field. Here, toxicity is internally referenced to a negative control (PBS) and a positive toxic control (the surfactant CTAB). Serial 2-fold dilutions of dendron were prepared from a stock solution, starting from 250 μg/mL in the 96-well microplate. As the positive toxicity control for 100% cell death, we employed the cationic surfactant molecule cetyltrimethylammonium bromide (CTAB), which is known to fully lyse HeLa cells. In this assay condition, CTAB exhibited a classical sigmoidal dose−response curve with an LC_{50} of 3.5 μg/mL, consistent with a highly cytotoxic substance. In comparison, $C_{14}G_2$ is cytotoxic (LC_{50} = 32 μg/mL), $C_{14}G_3$ is moderately cytotoxic (LC_{50} = 85 μg/mL) and C_2G_3 is completely nontoxic up to the highest concentration tested (LC_{50} > 250 μg/mL). When comparing these results to the HC_{50} data, it is important to recognize that the hemolysis assay only probes membrane disruption, whereas HeLa cells may undergo myriad mechanism(s) of cell death detectable by the metabolic assay. Although the LC_{50} values differ numerically from the HC_{50} results, they do follow the same general trend: C_2G_3 is nontoxic, $C_{14}G_3$ is moderately toxic, and $C_{14}G_2$ is the most toxic.

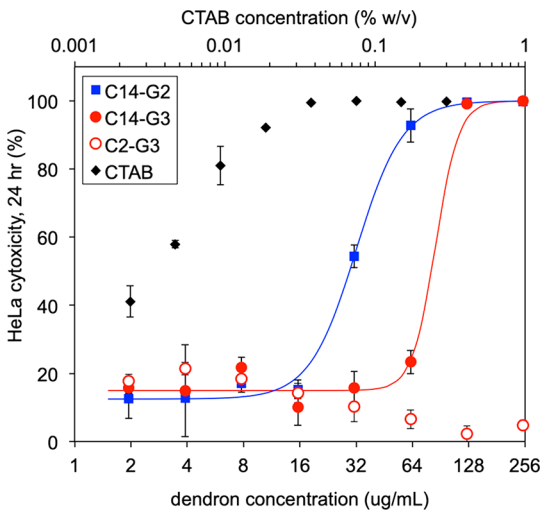

Figure 5. Cytotoxicity against HeLa cells.

Interestingly, the dose−response curve for the most hydrophobic third generation dendron, $C_{14}G_3$, undergoes a very sharp transition from nontoxic at 62.5 μg/mL to completely toxic at the next dilution, 125 μg/mL. Although the mechanism underpinning this unusually sharp transition is not entirely clear at present, one may speculate that the active toxic species at 125 μg/mL (above the CMC) represents the compound in the micellar form, whereas the individually solvated species are nontoxic, vide supra. It is well-known in the literature that polycationic nanoparticles, including PAMAM dendrimers of higher generation (G7, G8), are toxic to human cancer cells in vitro by a mechanism involving membrane translocation and apoptosis.[60] Although outside the scope of this work, one may speculate that the self-assembled micelles of the $C_{14}G_3$ dendron exert their cytotoxicity by a related mechanism.

***E. coli* Membrane Permeabilization.** Encouraged by the outstanding antibacterial performance and hemocompatibility displayed by the lead compound $C_{14}G_3$, we further endeavored to study the mechanism of action. Because this compound was

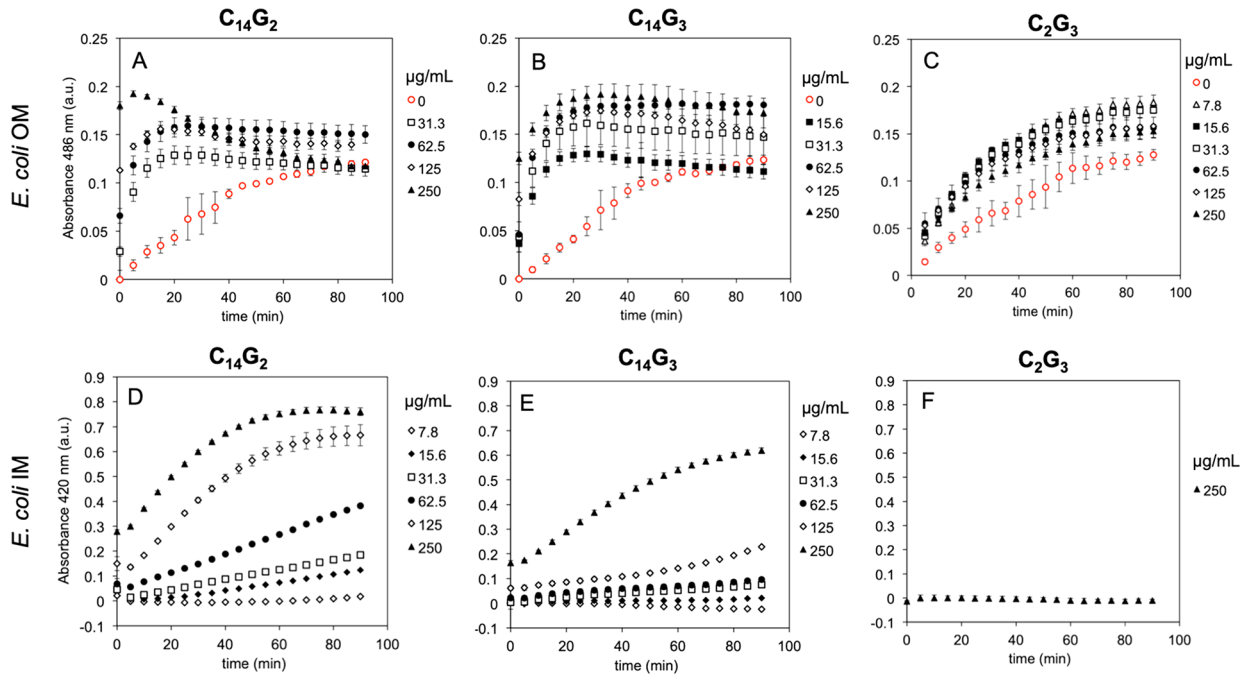

Figure 6. Leakage from *E. coli* (A−C) outer and (D−F) inner membranes induced by selected representative dendrons (A, D) $C_{14}G_2$, (B, E) $C_{14}G_3$, and (C, F) C_2G_3. For the OM leakage case, background permeabilization (in the absence of dendrons) is not trivial, as indicated by the red empty circles. The positive control for complete OM lysis, polymyxin B, gave a max absorbance value at 484 nm of 0.178 at 90 min. The positive control for IM lysis, CTAB, gave a max absorbance at 420 nm of 0.921 at 90 min.

https://dx.doi.org/10.1021/acsami.9b19076
ACS Appl. Mater. Interfaces XXXX, XXX, XXX−XXX

specifically designed to mimic the direct membrane disruption activity inherent to antimicrobial peptides, we first examined its ability to induce leakage across the inner and outer membranes (OM/IM) of *E. coli* cells.[61]

To measure the extent of the membrane permeabilization for *E. coli* outer (OM) and inner membranes (IMs), two independent enzymatic assays were employed in parallel. Nitrocefin is used to probe OM permeability as a substrate for the periplasmic enzyme β-lactamase; the IM integrity is probed by the cytoplasmic enzyme β-galactosidase, which is activated to react with *ortho*-nitrophenyl-β-galactoside (ONPG).[62] Typically, these enzymes and their substrates are not readily able to cross the membrane barrier. When the membrane integrity is compromised, however, the substrates are more readily able to access the enzyme, which leads to more rapid formation of the products. The formation of product is tracked by measuring the absorbance via UV/vis spectroscopy in 96-well microplate format.

We find that representative examples from the library of cationic dendrons in this work indeed exert membrane-lytic activity against the *E. coli* membranes. We selected C_2G_3 (inactive), $C_{14}G_2$ (biocidal), and $C_{14}G_3$ (selectively bactericidal) as model compounds for these assays. All three compounds permeabilize the OM in a time- and dose-dependent manner as compared to the background leakage signal (Figure 6). The $C_{14}G_2$ dendron lyses the OM more rapidly and at lower threshold concentrations compared to $C_{14}G_3$, which in turn lyses the OM faster than C_2G_3. The latter dendron, which contains the shortest alkyl chain, only slightly enhances OM permeability relative to baseline. In terms of the IM permeability, it appears that C_2G_3 (inactive) exerts almost no discernible effect compared to the background signal even at the highest concentration tested (250 μg/mL) over 90 min. On the other hand, both $C_{14}G_2$ (biocidal) and $C_{14}G_3$ (selectively bactericidal) strongly enhance the IM permeability. The most potent antibacterial in this library $C_{14}G_2$ shows rapid IM lysis at high concentrations (250 μg/mL) and gradual lysis at lower concentration (15.6 μg/mL). The most selective antibacterial compound in this library, $C_{14}G_3$, shows slower IM permeabilization relative to its second-generation counterpart with the same alkyl tail length at high concentration (250 μg/mL) and very gradual permeabilization at lower concentrations (down to 31 μg/mL). Thus, the correlation between membrane permeabilization activity and the observed differences in MIC values strongly suggest that membrane disruption is indeed a primary mode of direct action for these bactericidal agents.

Confocal Microscopy. We further examined the effect of the dendron $C_{14}G_3$ on bacterial cell viability and morphology using confocal laser scanning microscopy with a commercially available LIVE/DEAD staining kit. The stains are SYTO9 (green channel), which stains living *E. coli* and *S. aureus* cells, and propidium iodide (red channel), which emits strongly only upon intercalation into cytoplasmic DNA.[63] In control images of bacteria alone, with no dendron added, the SYTO-9 channel emits brightly and with high contrast, revealing the characteristic rod-shaped *E. coli* (Figure 7A, B) and spherical *S. aureus* cell morphologies (Figure 7E, F). Because PI is normally not membrane permeable, the live control cell images show no discernible red emission. Combined, these data show that the bacteria in the control conditions remain viable. Upon treatment with the cationic dendron (at a concentration of 4 × MIC, 32 μg/mL), however, the emission in the green channel is substantially displaced and the PI stain in the red channel appears with high contrast for both *E. coli* and *S. aureus*, suggesting that all cells visible in the image have been effectively killed by these antibacterial agents (Figure 7C, D, G, H). These findings lend further support to the notion that $C_{14}G_3$ kills bacterial cells directly and by a mechanism that is most likely dependent on membrane disruption.

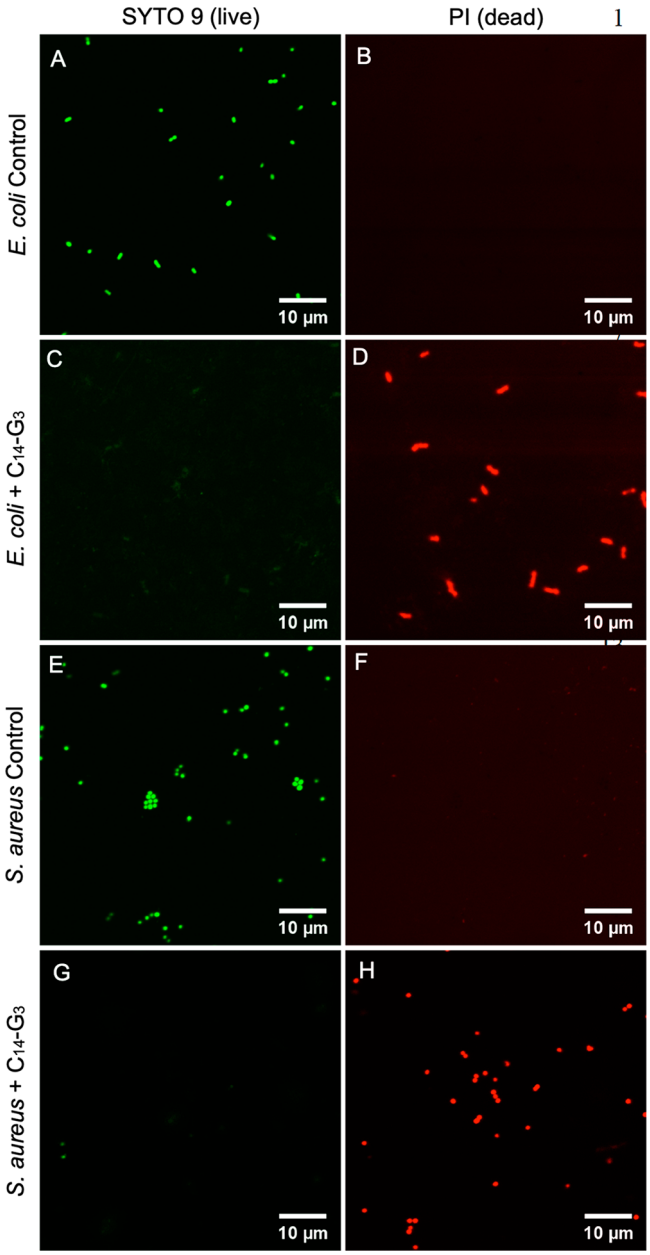

Figure 7. Confocal images of (A–D) *E. coli* and (E-H) *S. aureus* in the presence and absence of $C_{14}G_3$ at 4 × MIC. The green channel (SYTO9) indicates live cells and the red channel (PI) indicates dead cells.

Interestingly, the PI-stained *E. coli* cells treated with C_{14}-G_3 appear to have a somewhat abnormal morphology upon close examination (see the Supporting Information for full-scale image). In each case, the images revealed a distorted cell shape compared to the smooth rod-shaped control cells. The root cause for this observation is unclear at present, but one may speculate that the process involves polar localization of anionic phospholipids such as cardiolipin (CL).[64] Indeed, recent

https://dx.doi.org/10.1021/acsami.9b19076
ACS Appl. Mater. Interfaces XXXX, XXX, XXX−XXX

biophysical studies have shown that protein binding to CL is driven by electrostatic attraction combined with hydrophobic effects.[65] G. C. L. Wong and co-workers have shown that induction of negative Gaussian curvature in bacterial membrane bilayers is a powerful predictor of membrane-disrupting antibacterial activity.[66−68] Given the unique architecture of the molecular umbrellas in this work, one may reasonably speculate that $C_{14}G_3$ is well-suited for selective disruption of anionic phospholipid bilayers, perhaps via generation of negative Gaussian curvature. Future mechanistic studies that aim to elucidate the role of lipids in the membrane binding, curvature, and disruption activity of these dendrons are therefore warranted.

■ CONCLUSIONS

We developed the first combinatorial library of cationic molecular umbrella amphiphiles that display multivalent cationic charge on one face of the molecule and a centrally ensconced hydrophobic tail. The modular synthetic approach enabled facile access to a series of dendrons with precise and independently controlled cationic charge and hydrophobicity. In general, elongation of the hydrophobic alkyl chain monotonically enhances antibacterial activity in the first-, second-, and third-generation dendron series. Whereas the antibacterial activity had only weak dependence on generation number, the hemolytic activity was markedly sensitive to generation. All of the first-generation dendrons are categorized as biocidal agents with very little cell-type selectivity. The G2 series showed improved selectivity and the G3 series yielded an example compound with extremely high selectivity index value (HC_{50}/MIC = 1250). This remarkable outcome can be attributed to the precision design and synthesis of macromolecules that mimic not only the basic features of HDP composition, but also the segregated or clustered arrangement of cationic charge and hydrophobicity. We propose that the molecular umbrella design effectively promotes interfacial localization of the dendrons on bacterial biomembranes and subsequent membrane disruption. The most selective compound from our library screen, a third-generation dendron bearing eight cationic groups and a 14-carbon alkyl chain, was carried forward for more in-depth studies. The compound is a rapid and broad-spectrum bactericidal agent, which efficiently permeabilized *E. coli* cell inner and outer membranes in a time- and dose-dependent manner. The results presented here highlight the utility of a molecular design principle that is focused on the propensity of macromolecules to adopt conformations that favor selective interaction with bacterial biomembranes.

■ EXPERIMENTAL METHODS

Materials. Reagents and reactants were purchased commercially and used as received without further purification unless otherwise noted. 2,2′-bis(hydroxymethyl)propionic acid (bis-MPA), 2,2-dimethoxypropane, *p*-toluenesulfonic monohydrate, *β*-alanine, di-*tert*-butyl dicarbonate (Boc anhydride), *N*,*N*′-dicyclohexylcarbodiimide (DCC), 4-dimethylaminopyridine (DMAP), ethanol, 1-butanol, 1-hexanol, 1-octanol, 1-decanol, 1-tetradecanol, and DOWEX-50WX2 gels were purchased from Sigma-Aldrich. Solvents acetone, CH_2Cl_2 (both regular and anhydrous), methanol, ethyl acetate, hexane and dioxane were also provided by Sigma-Aldrich. HCl (37%) and NH_4OH (25%) were obtained from Fisher. Silica gel (Sigma) for column chromatography was used to purify the products, during which thin-layer chromatography was performed on IB2-F J.T. Baker silica gel TLC (Germany) to track the process of purification. Phosphate-buffered saline (PBS) tablets, pyrene, and deuterated solvent were obtained from Sigma. Standard 1 N HCl and NaOH solution were purchased from Fisher. Bacterial strains *S. aureus* (ATCC25923). *E. coli* (ATCC 25922), methicillin-resistant *S. aureus* (MRSA, ATCC 33591), *Acinetobacter baumannii* (*A. baumannii* ATCC 17978), *Pseudomonas aeruginosa* (*P. aeruginosa*, ATCC 27853), *Enterococcus faecalis* (*E. faecalis*, ATCC 29212) were tested. Mueller Hinton (MH), tryptic soy, and brain heart infusion broth and agar were purchased from BD. Sterile PBS were prepared by dissolving one PBS tablet (Sigma) into 200 mL of water. The above growth media were sterilized by autoclaving at 121 °C for 20 min, stored at 4 °C, and used within 1 month. Sheep red blood cells (RBC) (10% suspension) were provided by MP Biomedicals, stored at 4 °C, and used before expiration. Live/dead Baclight stain was purchased from Thermo Fisher and prepared according to the instruction manual.

Nuclear Magnetic Resonance (NMR). ^{1}H NMR spectra were performed on a Varian 500 MHz NMR at 25 °C and chemical shifts (δ) were reported in parts per million (ppm). The spectra were referenced to residual solvent signals ($CDCl_3$ (δ = 7.26 ppm) and DMSO-d6 (δ = 2.50 ppm)). Spectra are expressed as chemical shifts, multiplicity (s = singlet, d = doublet, t = triplet, q = quartet, m = multiplet and/or multiple resonances, br = broad) and integration. ^{13}C NMR spectra were performed on a Bruker 600 MHz NMR also at 25 °C. The spectra were referenced to residual solvent signals ($CDCl_3$ (δ 77.0) and DMSO-d6 (δ 39.51), and expressed as chemical shifts

Pyrene Emission. Fluorescence spectroscopy of pyrene was measured on a Molecular Devices SpectraMax M2 multimode microplate spectrophotometer. A series of serial 2-fold dilutions of dendron solution, rangin from from 50 mg/mL to 39.1 μg/mL, were prepared in water. Ten microliters of the above dilutions was added to each well of a black 96-well plate and 90 μL of the pyrene-saturated PBS solution was then added to each well and thoroughly mixed. The final compound concentration on the microplate thus ranges from 5 mg/mL down to 3.9 μg/mL. The fluorescence emission from each well was measured, with excitation wavelength set at 334 nm and emission at 373 (I_1) and 384 nm (I_3) recorded. The quotient of I_1/I_3 was plotted against the concentration of the dendrons in a semilog plot and curve-fitting was done with the empirical Hill equation.

Dynamic Light Scattering (DLS). DLS was performed on an Anton Paar Litesizer 500 instrument operating at 90° geometry. PBS buffer filtered through a 1 um glass fiber syringe was used for the preparation of solutions. A stock solution of $C_{14}G_3$ at 5 mg/mL in PBS was prepared with vortexing at 1500 rpm for 5 min. Solutions at 0.25, 0.05, 0.025, and 0.0125 mg/mL were prepared by successive dilutions and were vortexed for an additional 5 min. The samples were loaded in PS cuvettes and measured at 20 °C. The CONTIN algorithm was employed for the analysis of the autocorrelation function.

Potentiometric Titration. The pH of the dendron solution during titration was monitored by a Mettler Toledo SevenCompact pH meter. Dendron (15 mg) was dissolved in 150 mM NaCl solution (15 mL). The solution was purged with nitrogen for 15 min and maintained through the titration to avoid the influence of dissolved CO_2. Standard 1N NaOH solution (2 μL aliquots) were then inject via glass microsyringe to the solution with vigorous stirring and the pH was measured after stabilization for 2 min. The titration continued until pH reached 9.5 to avoid hydrolysis of the dendrons. Back titration was performed with the addition of standard 1 N HCl solution (2 μL) until the pH reached ≤7.5. The pH was plotted against the degree of ionization of the amine groups α according to the following equation:

$$\alpha = \frac{NH_3^+]}{[-NH_3^+] + [-NH_2]} = \frac{[Cl^-] + [TFA^-] + [OH^-] - [Na^+] - [H^+]}{[-NH_3^+] + [-NH_2]} \quad (1)$$

General Procedures for the Synthesis of Dendrons. The dendrons with hydroxyl surface groups were synthesized according to

https://dx.doi.org/10.1021/acsami.9b19076
ACS Appl. Mater. Interfaces XXXX, XXX, XXX−XXX

the route in Scheme 1. Acetonide bis-MPA[69] and Boc-β-alanine[70] were prepared according to previously reported procedures. For the synthesis of poly(bis-MPA) dendron cores, generally, to each 1 equiv. of hydroxyl group (either alcohol or poly(bis-MPA) dendrons), 1.2 equiv. of acetonide bis-MPA, and 0.2 equiv. of 4-dimethylaminopyridine (DMAP) were mixed in dry CH_2Cl_2; 1.2 equiv. of DCC was dissolved in CH_2Cl_2 and added dropwise into the above solution submerged in ice bath. After stirring at room temperature overnight, the crude product was concentrated and purified through column chromatography. The deprotection of acetonide group was conducted using DOWEX-50WX2 gels in methanol at 50 °C overnight. The product was obtained by filtration of the gels and evaporation of methanol. The attachment of Boc-β-alanine to the peripheral hydroxy groups used the same protocol as the acetonide bis-MPA. The deprotection of the Boc groups was conducted by dissolving 0.5 g dendrons in 5 mL of TFA and stirred at room temperature for 1 h. After evaporation and lyophilization, the final product was achieved. Detailed synthesis processes and characterizations of each dendron are presented in the Supporting Information.

Minimum Inhibitory Concentration (MIC). Stock solutions (20 mg/mL) were prepared by dissolving each dendron in Milli-Q water. Then, 2-fold serial dilutions were conducted to cover the range of concentration from 10 mg/mL to 0.25 μg/mL. Bacteria were first streaked on MH agar plates and incubated at 37 °C overnight. One colony was picked and inoculated in 10 mL of MH broth and incubated at 37 °C on a shaker at 500 rpm overnight. The overnight culture was diluted using MH broth until OD_{600} reached 0.1 and incubated for another 90 min to reach mid log phase. The culture at mid log phase was then diluted again using MH broth until OD_{600} was 0.1 (~5×10^7 CFU/mL for *E. coli* and ~6×10^7 CFU/mL for *S. aureus*). The culture was diluted by a factor of 1×10^2 to afford the density of *E. coli* at around 5×10^5 CFU/mL and *S. aureus* at 6×10^5 CFU/mL. Ten microliters of the dilutions of dendron solutions were added into 96-well plates, and then 90 μL of the final culture was added and mixed. The 96-well plates were sealed with parafilm and incubated at 37 °C overnight. The lowest concentration of the dendron solution that inhibit visual growth of bacteria is the minimum inhibitory concentration. All tests were performed three times in triplicate.

Hemolysis Assay. Ten percent sheep RBC suspension was centrifuged (2000 rpm, 5 min) and washed with PBS three times. The washed RBCs were resuspended in 10 mL PBS to reach 1% RBC suspension. To each well of the round-bottom 96-well plate, 10 μL of the dendron solutions were added. To the wells of positive control was added 10 μL 0.1% *v/v* Triton X solution, and to the negative control wells was added 10 μL of PBS. Ninety microliters of the 1% RBC suspension in PBS was then mixed with the dendron solution. The 96-well plate was sealed with parafilm and incubated at 37 °C for 1 h agitated at 200 rpm to avoid the deposit of RBCs. After incubation, the plate was centrifuged at 1000 rpm for 10 min. Ten microliters of supernatant of each well was transferred into a flat-bottom 96-well plate and diluted with 90 μL of PBS. The absorbance of each well was measured at 415 nm. The percentage of hemolysis (H) was calculated using the equation below:

$$H(\%) = \frac{OD_{415}(\text{Dendron}) - OD_{415}(\text{PBS})}{OD_{415}(\text{TritonX}) - OD_{415}(\text{PBS})} 100\% \quad (2)$$

HC_{50} was calculated as the concentration of dendrons causing 50% hemolysis by fitting the data with function

$$H = \frac{1}{1 + \frac{HC_{50}}{[C_nG_x]^n}} \quad (3)$$

where HC_{50} and n are the curve-fitting variables that represent the characteristic hemolytic concentration and the Hill coefficient (indicative of the steepness of the dose−response transition). All tests were performed three times in triplicate.

Confocal Microscopy. A suspension of *S. aureus* or *E. coli* at mid log phase was obtained through the same procedure described in MIC assay. The bacteria were washed with PBS three times, resuspended in PBS and adjusted to OD_{600} = 0.1. Two $C_{14}G_3$ aqueous solutions were prepared with concentrations respectively at 320 and 160 μg/mL. Forty microliters of the 320 μg/mL dendron solution was added into 3.6 mL *E. coli* suspension to reach the final concentration of dendron at 32 μg/mL (4 × MIC). Similarly, 40 μL of the 160 μg/mL dendron solution was added into 3.6 mL of *S. aureus* suspension. The suspensions were incubated at 37 °C agitated at 500 rpm for 3 h. Bacteria were pelleted at 2000 rpm for 10 min and resuspended in 100 μL of PBS. The above suspension was stained with Live/Dead Baclight Stain according to the instruction manual. Five μL of the stained suspension was trapped between a glass slide and coverslip and observed under a Zeiss LSM 510 Meta laser scanning confocal microscope. SYTO9 was excited using Argon laser (488 nm) and its emission at 510−540 nm was recorded. Propidium iodide was excited using HeNe1 laser (543 nm) and emission at 620−650 nm was recorded. Images were taken in 1024 × 1024 pixel format.

Bactericidal Kinetics. Two 4.5 mL *E. coli* suspensions at mid log phase with ~5E5 CFU/mL density were prepared according to the same procedure described in MIC assay. Fifty microliters of 160 μg/mL G3-β-alanine TFA was respectively added to the one of the 4.5 mL *E. coli* suspension to reach the final dendron concentration at 16 μg/mL (2 × MIC). In another suspension was added 50 μL water as control. For every 5−10 min, an aliquot of 100 μL of suspension was taken out, serially diluted (10-fold), and spread on MH agar plates. The plates were incubated overnight and the colonies were counted to plot the CFU of bacteria against time.

Cytotoxicity. Cytotoxicity of dendrons was evaluated in HeLa cells as assayed by CellTiter-Blue reagent from Promega. In this assay, active cellular metabolism is measured by the enzymatic conversion of Resarzurin to Resorufin (florescent at 590 nm). HeLa cells were seeded into a 96-well flat bottom cell culture plate at 100,000 cells per well and grown for 24 h in 180 μL of DMEM 10% FBS, 1% Pen/Strep, 1% L-Glut. After 24 h, cells were exposed to various concentrations of dendrons (C_2G_3, $C_{14}G_2$, and $C_{14}G_3$) beginning at 250 μg/mL final concentration and serially diluted in water 2-fold to ~2 μg/mL. As a positive control for cytotoxicity, CTAB reagent was used at 0.3% (completely cytotoxic) and also serially diluted 2-fold to 0.0002% final concentration. Addition of 20 μL of water was used as a negative control. Plates were incubated in a standard CO_2 incubator 5% CO_2 37 °C for 24 h. Following 24 h of incubation with dendrons, 20 μL of CellTiter-Blue reagent was added directly to plate, mixed and incubated at 37 °C for 2 h and analyzed on Synergy HT florescent plate reader with Ex. λ = 485 nm, Em. λ = 590 nm. All three dendron samples were tested in triplicate, CTAB was performed in duplicate.

***E. coli* Outer Membrane Permeabilization Assay.** A single colony of *E. coli* D31 was transferred into LB broth containing 100 μg/mL ampicillin (LB-Amp) followed by incubation at 37°C with shaking for 18 h. The overnight culture was diluted 1:250 in fresh LB-Amp. The diluted culture was placed in a shaking incubator set at 37°C until OD_{600} of the culture reached 0.2−0.6. At this point, the culture was centrifuged at 2500 rpm for 15 min in a benchtop clinical centrifuge. The supernatant was discarded and the pellet was resuspended in PBS to achieve a bacterial cell density of 2×10^8 CFU/ml. The nitrocefin stock solution was prepared dissolving 1 mg of nitrocefin in 100 μL DMSO, which was subsequently diluted to 2.0 mL with PBS to achieve a final stock concentration of 500 μg/mL. Nitrocefin solution was covered in aluminum foil and stored at 4°C before dispensing into plates. Solutions were dispensed into a 96 well plate in the subsequent order: 10 μL of polymer or control molecule with serial dilutions in water starting from 250 μg/mL final concentration in the well, 80 μL of *E. coli* suspension, and 10 μL of 500 μg/mL nitrocefin. Following the addition of nitrocefin to the wells, the absorbance was immediately recorded at 486 nm and was recorded every 5 min over the next 90 min with shaking between readings.

***E. coli* Inner Membrane Permeabilization Assay.** A single colony of *E. coli* D31 was transferred into 3 mL of LB broth. The overnight culture was diluted 1:250 in 20 mL of LB containing 100

https://dx.doi.org/10.1021/acsami.9b19076
ACS Appl. Mater. Interfaces XXXX, XXX, XXX−XXX

μL of 100 mM isopropyl β-D-1-thiogalactopyranoside (IPTG) to induce expression of the galactosidase gene. The diluted culture was placed in a shaking incubator set at 37°C until OD_{600} of the culture reached ~0.2. The following solutions were transferred into each well of a 96 well plate in the order listed: 56 μL of Z-buffer, 10 μL of serially diluted polymers starting from 250 μg/mL, 19 μL of *E. coli* culture, and 15 μL of 4 mg/mL *o*-nitrophenyl-β-galactoside (ONPG) in Z-buffer. Immediately after ONPG addition, absorbance was recorded at 420 nm every 5 min for 90 min with shaking in between readings.

■ ASSOCIATED CONTENT

Supporting Information

The Supporting Information is available free of charge at https://pubs.acs.org/doi/10.1021/acsami.9b19076.

Detailed materials and methods, synthetic procedures, NMR spectra, and additional experimental details (PDF)

■ AUTHOR INFORMATION

Corresponding Author

Edmund F. Palermo − *Rensselaer Polytechnic Institute, Troy, New York;* orcid.org/0000-0003-3656-787X; Email: palere@rpi.edu

Other Authors

Ao Chen − *Rensselaer Polytechnic Institute, Troy, New York*

Apostolos Karanastasis − *Rensselaer Polytechnic Institute, Troy, New York;* orcid.org/0000-0001-9966-7873

Kaitlyn R. Casey − *Rowan University, Glassboro, New Jersey*

Matthew Necelis − *Rowan University, Glassboro, New Jersey*

Benjamin R. Carone − *Rowan University, Glassboro, New Jersey*

Gregory A. Caputo − *Rowan University, Glassboro, New Jersey*

Complete contact information is available at: https://pubs.acs.org/10.1021/acsami.9b19076

Notes

The authors declare the following competing financial interest(s): E.F.P. and A.C. are co-inventors on a provisional patent application disclosing the use of these dendrons as disinfectants.

■ ACKNOWLEDGMENTS

The authors gratefully acknowledge Prof. Chang Ryu and Prof. R. Helen Zha for assistance with DLS measurements. E.F.P. acknowledges support from a 3M Non-Tenured Faculty Award and a National Science Foundation CAREER Award (#1653418). B.R.C. acknowledges seed funding from Rowan University. Acknowledgment is made to the Donors of the American Chemical Society Petroleum Research Fund for partial support of this research (for A.C.).

■ REFERENCES

(1) Matyjaszewski, K. Architecturally Complex Polymers with Controlled Heterogeneity. *Science* **2011**, *333* (6046), 1104−1105.

(2) Gutekunst, W. R.; Hawker, C. J. A General Approach to Sequence-Controlled Polymers Using Macrocyclic Ring Opening Metathesis Polymerization. *J. Am. Chem. Soc.* **2015**, *137* (25), 8038−8041.

(3) McHale, R.; Patterson, J. P.; Zetterlund, P. B.; O'Reilly, R. K. Biomimetic Radical Polymerization via Cooperative Assembly of Segregating Templates. *Nat. Chem.* **2012**, *4* (6), 491−497.

(4) Badi, N.; Lutz, J. F. Sequence Control in Polymer Synthesis. *Chem. Soc. Rev.* **2009**, *38* (12), 3383−3390.

(5) Barnes, J. C.; Ehrlich, D. J. C.; Gao, A. X.; Leibfarth, F. A.; Jiang, Y. V.; Zhou, E.; Jamison, T. F.; Johnson, J. A. Iterative Exponential Growth of Stereo- and Sequence-controlled Polymers. *Nat. Chem.* **2015**, *7* (10), 810−815.

(6) Leibfarth, F. A.; Mattson, K. M.; Fors, B. P.; Collins, H. A.; Hawker, C. J. External Regulation of Controlled Polymerizations. *Angew. Chem., Int. Ed.* **2013**, *52* (1), 199−210.

(7) Szwarc, M. Replica Polymerization. *J. Polym. Sci.* **1954**, *13* (69), 317−318.

(8) Szwarc, M. Living Polymers. *Nature* **1956**, *178* (4543), 1168−1169.

(9) Lutz, J.-F.; Ouchi, M.; Liu, D. R.; Sawamoto, M. Sequence-Controlled Polymers. *Science* **2013**, *341* (6146), 1238149.

(10) Kamigaito, M.; Ando, T.; Sawamoto, M. Metal-catalyzed Living Radical Polymerization. *Chem. Rev.* **2001**, *101* (12), 3689−3745.

(11) Kramer, J. W.; Treitler, D. S.; Dunn, E. W.; Castro, P. M.; Roisnel, T.; Thomas, C. M.; Coates, G. W. Polymerization of Enantiopure Monomers Using Syndiospecific Catalysts: A New Approach To Sequence Control in Polymer Synthesis. *J. Am. Chem. Soc.* **2009**, *131* (44), 16042−16044.

(12) Connor, R. E.; Tirrell, D. A. Non-canonical Amino Acids in Protein Polymer Design. *Polym. Rev.* **2007**, *47* (1), 9−28.

(13) Zasloff, M. Antimicrobial Peptides of Multicellular Organisms. *Nature* **2002**, *415* (6870), 389−395.

(14) Brogden, K. A. Antimicrobial Peptides: Pore Formers or Metabolic Inhibitors in Bacteria? *Nat. Rev. Microbiol.* **2005**, *3* (3), 238−250.

(15) Hilchie, A. L.; Wuerth, K.; Hancock, R. E. W. Immune Modulation by Multifaceted Cationic Host Defense (Antimicrobial) Peptides. *Nat. Chem. Biol.* **2013**, *9* (12), 761−768.

(16) Ergene, C.; Yasuhara, K.; Palermo, E. F. Biomimetic Antimicrobial Polymers: Recent Advances in Molecular Design. *Polym. Chem.* **2018**, *9* (18), 2407−2427.

(17) Konai, M. M.; Bhattacharjee, B.; Ghosh, S.; Haldar, J. Recent Progress in Polymer Research to Tackle Infections and Antimicrobial Resistance. *Biomacromolecules* **2018**, *19* (6), 1888−1917.

(18) Takahashi, H.; Caputo, G. A.; Vemparala, S.; Kuroda, K. Synthetic Random Copolymers as a Molecular Platform To Mimic Host-Defense Antimicrobial Peptides. *Bioconjugate Chem.* **2017**, *28* (5), 1340−1350.

(19) Tew, G. N.; Scott, R. W.; Klein, M. L.; Degrado, W. F. De Novo Design of Antimicrobial Polymers, Foldamers, and Small Molecules: From Discovery to Practical Applications. *Acc. Chem. Res.* **2010**, *43* (1), 30−39.

(20) Chakraborty, S.; Liu, R.; Hayouka, Z.; Chen, X.; Ehrhardt, J.; Lu, Q.; Burke, E.; Yang, Y.; Weisblum, B.; Wong, G. C. L.; Masters, K. S.; Gellman, S. H. Ternary Nylon-3 Copolymers as Host-Defense Peptide Mimics: Beyond Hydrophobic and Cationic Subunits. *J. Am. Chem. Soc.* **2014**, *136* (41), 14530−14535.

(21) Horne, W. S.; Gellman, S. H. Foldamers with Heterogeneous Backbones. *Acc. Chem. Res.* **2008**, *41* (10), 1399−1408.

(22) Mowery, B. P.; Lee, S. E.; Kissounko, D. A.; Epand, R. F.; Epand, R. M.; Weisblum, B.; Stahl, S. S.; Gellman, S. H. Mimicry of Antimicrobial Host-defense Peptides by Random Copolymers. *J. Am. Chem. Soc.* **2007**, *129* (50), 15474−15476.

(23) Palermo, E. F.; Lee, D. K.; Ramamoorthy, A.; Kuroda, K. Role of Cationic Group Structure in Membrane Binding and Disruption by Amphiphilic Copolymers. *J. Phys. Chem. B* **2011**, *115* (2), 366−375.

(24) Kuroda, K.; DeGrado, W. F. Amphiphilic Polymethacrylate Derivatives as Antimicrobial Agents. *J. Am. Chem. Soc.* **2005**, *127* (12), 4128−4129.

(25) Porel, M.; Thornlow, D. N.; Phan, N. N.; Alabi, C. A. Sequence-defined Bioactive Macrocycles via an Acid-catalysed Cascade Reaction. *Nat. Chem.* **2016**, *8* (6), 590−596.

(26) Song, A. R.; Walker, S. G.; Parker, K. A.; Sampson, N. S. Antibacterial Studies of Cationic Polymers with Alternating, Random, and Uniform Backbones. *ACS Chem. Biol.* **2011**, *6* (6), 590−599.

(27) Zhou, Z.; Ergene, C.; Lee, J. Y.; Shirley, D. J.; Carone, B. R.; Caputo, G. A.; Palermo, E. F. Sequence and Dispersity Are Determinants of Photodynamic Antibacterial Activity Exerted by Peptidomimetic Oligo(thiophene)s. *ACS Appl. Mater. Interfaces* **2019**, *11* (2), 1896−1906.

(28) Gabriel, G. J.; Tew, G. N. Conformationally Rigid Proteomimetics: A Case Study in Designing Antimicrobial Aryl Oligomers. *Org. Biomol. Chem.* **2008**, *6* (3), 417−423.

(29) Wang, Z. APD: the Antimicrobial Peptide Database. *Nucleic Acids Res.* **2004**, *32*, D590−D592.

(30) Punia, A.; Lee, K.; He, E.; Mukherjee, S.; Mancuso, A.; Banerjee, P.; Yang, N. L. Effect of Relative Arrangement of Cationic and Lipophilic Moieties on Hemolytic and Antibacterial Activities of PEGylated Polyacrylates. *Int. J. Mol. Sci.* **2015**, *16* (10), 23867−23880.

(31) Engler, A. C.; Tan, J. P. K.; Ong, Z. Y.; Coady, D. J.; Ng, V. W. L.; Yang, Y. Y.; Hedrick, J. L. Antimicrobial Polycarbonates: Investigating the Impact of Balancing Charge and Hydrophobicity Using a Same-Centered Polymer Approach. *Biomacromolecules* **2013**, *14* (12), 4331−4339.

(32) Sambhy, V.; Peterson, B. R.; Sen, A. Antibacterial and Hemolytic activities of Pyridinium Polymers as a Function of the Spatial Relationship Between the Positive Charge and the Pendant Alkyl Tail. *Angew. Chem., Int. Ed.* **2008**, *47* (7), 1250−1254.

(33) Mowery, B. P.; Lindner, A. H.; Weisblum, B.; Stahl, S. S.; Gellman, S. H. Structure-activity Relationships among Random Nylon-3 Copolymers That Mimic Antibacterial Host-Defense Peptides. *J. Am. Chem. Soc.* **2009**, *131* (28), 9735−9745.

(34) Palermo, E. F.; Sovadinova, I.; Kuroda, K. Structural Determinants of Antimicrobial Activity and Biocompatibility in Membrane-Disrupting Methacrylamide Random Copolymers. *Biomacromolecules* **2009**, *10* (11), 3098−3107.

(35) Palermo, E. F.; Kuroda, K. Chemical Structure of Cationic Groups in Amphiphilic Polymethacrylates Modulates the Antimicrobial and Hemolytic Activities. *Biomacromolecules* **2009**, *10* (6), 1416−1428.

(36) Lienkamp, K.; Madkour, A. E.; Musante, A.; Nelson, C. F.; Nuesslein, K.; Tew, G. N. Antimicrobial Polymers Prepared by ROMP with Unprecedented Selectivity: A Molecular Construction Kit Approach. *J. Am. Chem. Soc.* **2008**, *130* (30), 9836−9843.

(37) Rahman, M. A.; Bam, M.; Luat, E.; Jui, M. S.; Ganewatta, M. S.; Shokfai, T.; Nagarkatti, M.; Decho, A. W.; Tang, C. B. Macromolecular-clustered Facial Amphiphilic Antimicrobials. *Nat. Commun.* **2018**, *9*, 5231.

(38) Janout, V.; Bienvenu, C.; Schell, W.; Perfect, J. R.; Regen, S. L. Molecular Umbrella-Amphotericin B Conjugates. *Bioconjugate Chem.* **2014**, *25* (8), 1408−1411.

(39) Janout, V.; Lanier, M.; Regen, S. L. Molecular Umbrellas. *J. Am. Chem. Soc.* **1996**, *118* (6), 1573−1574.

(40) Buhleier, E.; Wehner, W.; Vogtle, F. Cascade-Chain-Like and Nonskid-Chain-Like Syntheses of Molecular Cavity Topologies. *Synthesis* **1978**, *1978* (2), 155−158.

(41) Smith, D. K.; Muller, L. Dendritic Biomimicry: Microenvironmental Effects on Tryptophan Fluorescence. *Chem. Commun.* **1999**, No. 18, 1915−1916.

(42) Balogh, L.; Swanson, D. R.; Tomalia, D. A.; Hagnauer, G. L.; McManus, A. T. Dendrimer−Silver Complexes and Nanocomposites as Antimicrobial Agents. *Nano Lett.* **2001**, *1* (1), 18−21.

(43) Wu, G.; Barth, R. F.; Yang, W.; Chatterjee, M.; Tjarks, W.; Ciesielski, M. J.; Fenstermaker, R. A. Site-Specific Conjugation of Boron-Containing Dendrimers to Anti-EGF Receptor Monoclonal Antibody Cetuximab (IMC-C225) and Its Evaluation as a Potential Delivery Agent for Neutron Capture Therapy. *Bioconjugate Chem.* **2004**, *15* (1), 185−194.

(44) Nardin, E. H.; Calvo-Calle, J. M.; Oliveira, G. A.; Nussenzweig, R. S.; Schneider, M.; Tiercy, J.-M.; Loutan, L.; Hochstrasser, D.; Rose, K. A Totally Synthetic Polyoxime Malaria Vaccine Containing Plasmodium falciparum B Cell and Universal T Cell Epitopes Elicits Immune Responses in Volunteers of Diverse HLA TypesContaining Plasmodium falciparum B Cell and Universal T Cell Epitopes Elicits Immune Responses in Volunteers of Diverse HLA Types. *J. Immunol.* **2001**, *166* (1), 481−489.

(45) Tam, J. P. Synthetic Peptide Vaccine Design: Synthesis and Properties of a High-density Multiple Antigenic Peptide System. *Proc. Natl. Acad. Sci. U. S. A.* **1988**, *85* (15), 5409−5413.

(46) Charles, S.; Vasanthan, N.; Kwon, D.; Sekosan, G.; Ghosh, S. Surface Modification of Poly(amidoamine) (PAMAM) Dendrimer as Antimicrobial Agents. *Tetrahedron Lett.* **2012**, *53* (49), 6670−6675.

(47) Chen, C. Z. S.; Beck-Tan, N. C.; Dhurjati, P.; van Dyk, T. K.; LaRossa, R. A.; Cooper, S. L. Quaternary Ammonium Functionalized Poly(Propylene Imine) Dendrimers as Effective Antimicrobials: Structure-Activity Studies. *Biomacromolecules* **2000**, *1* (3), 473−480.

(48) Calabretta, M. K.; Kumar, A.; McDermott, A. M.; Cai, C. Antibacterial Activities of Poly(amidoamine) Dendrimers Terminated with Amino and Poly(ethylene glycol) Groups. *Biomacromolecules* **2007**, *8* (6), 1807−1811.

(49) Mintzer, M. A.; Grinstaff, M. W. Biomedical Applications of Dendrimers: A Tutorial. *Chem. Soc. Rev.* **2011**, *40* (1), 173−190.

(50) Xu, L. L.; He, C.; Hui, L. W.; Xie, Y. T.; Li, J. M.; He, W. D.; Yang, L. H. Bactericidal Dendritic Polycation Cloaked with Stealth Material via Lipase-Sensitive Intersegment Acquires Neutral Surface Charge without Losing Membrane-Disruptive Activity. *ACS Appl. Mater. Interfaces* **2015**, *7* (50), 27602−27607.

(51) Lam, S. J.; O'Brien-Simpson, N. M.; Pantarat, N.; Sulistio, A.; Wong, E. H. H.; Chen, Y. Y.; Lenzo, J. C.; Holden, J. A.; Blencowe, A.; Reynolds, E. C.; Qiao, G. G. Combating Multidrug-resistant Gram-negative Bacteria with Structurally Nanoengineered Antimicrobial Peptide Polymers. *Nat. Microbiol.* **2016**, *1* (11), 16162.

(52) Kannan, R.; Prabakaran, P.; Basu, R.; Pindi, C.; Senapati, S.; Muthuvijayan, V.; Prasad, E. Mechanistic Study on the Antibacterial Activity of Self-Assembled Poly(aryl ether)-Based Amphiphilic Dendrimers. *ACS Appl. Bio Mater.* **2019**, *2* (8), 3212−3224.

(53) Antoni, P.; Robb, M. J.; Campos, L.; Montanez, M.; Hult, A.; Malmström, E.; Malkoch, M.; Hawker, C. J. Pushing the Limits for Thiol−Ene and CuAAC Reactions: Synthesis of a 6th Generation Dendrimer in a Single Day. *Macromolecules* **2010**, *43* (16), 6625−6631.

(54) Feliu, N.; Walter, M. V.; Montanez, M. I.; Kunzmann, A.; Hult, A.; Nystrom, A.; Malkoch, M.; Fadeel, B. Stability and Biocompatibility of a Library of Polyester Dendrimers in Comparison to Polyamidoamine Dendrimers. *Biomaterials* **2012**, *33* (7), 1970−1981.

(55) Stenström, P.; Hjorth, E.; Zhang, Y.; Andrén, O. C. J.; Guette-Marquet, S.; Schultzberg, M.; Malkoch, M. Synthesis and in vitro Evaluation of Monodisperse Amino-Functional Polyester Dendrimers with Rapid Degradability and Antibacterial Properties. *Biomacromolecules* **2017**, *18* (12), 4323−4330.

(56) Fukushima, K.; Tan, J. P. K.; Korevaar, P. A.; Yang, Y. Y.; Pitera, J.; Nelson, A.; Maune, H.; Coady, D. J.; Frommer, J. E.; Engler, A. C.; Huang, Y.; Xu, K. J.; Ji, Z. K.; Qiao, Y.; Fan, W. M.; Li, L. J.; Wiradharma, N.; Meijer, E. W.; Hedrick, J. L. Broad-Spectrum Antimicrobial Supramolecular Assemblies with Distinctive Size and Shape. *ACS Nano* **2012**, *6* (10), 9191−9199.

(57) Goddard, E. D.; Turro, N. J.; Kuo, P. L.; Ananthapadmanabhan, K. P. Fluorescence Probes for Critical Micelle Concentration Determination. *Langmuir* **1985**, *1* (3), 352−355.

(58) Hollmann, A.; Martinez, M.; Maturana, P.; Semorile, L. C.; Maffia, P. C., Antimicrobial Peptides: Interaction With Model and Biological Membranes and Synergism With Chemical Antibiotics. *Front. Chem.* **2018**, *6*, DOI: 10.3389/fchem.2018.00204.

(59) Palermo, E. F.; Vemparala, S.; Kuroda, K. Cationic Spacer Arm Design Strategy for Control of Antimicrobial Activity and Conformation of Amphiphilic Methacrylate Random Copolymers. *Biomacromolecules* **2012**, *13* (5), 1632−1641.
(60) Banaszak Holl, M. M.; Dougherty, C. A.; Vaidyanathan, S. Tailoring Dendrimer Conjugates for Biomedical Applications: The Impact of Altering Hydrophobicity. *J. Nanopart. Res.* **2018**, *20* (10), 284.
(61) Kohn, E. M.; Shirley, D. J.; Arotsky, L.; Picciano, A. M.; Ridgway, Z.; Urban, M. W.; Carone, B. R.; Caputo, G. A. Role of Cationic Side Chains in the Antimicrobial Activity of C18G. *Molecules* **2018**, *23*, 329.
(62) Mensa, B.; Kim, Y. H.; Choi, S.; Scott, R.; Caputo, G. A.; DeGrado, W. F. Antibacterial Mechanism of Action of Arylamide Foldamers. *Antimicrob. Agents Chemother.* **2011**, *55* (11), 5043−5053.
(63) Stocks, S. M. Mechanism and Use of the Commercially Available Viability Stain, BacLight. *Cytometry* **2004**, *61A* (2), 189−195.
(64) Oliver, P. M.; Crooks, J. A.; Leidl, M.; Yoon, E. J.; Saghatelian, A.; Weibel, D. B. Localization of Anionic Phospholipids in Escherichia coli Cells. *J. Bacteriol.* **2014**, *196* (19), 3386−3398.
(65) Planas-Iglesias, J.; Dwarakanath, H.; Mohammadyani, D.; Yanamala, N.; Kagan, V. E.; Klein-Seetharaman, J. Cardiolipin Interactions with Proteins. *Biophys. J.* **2015**, *109* (6), 1282−1294.
(66) Hu, K.; Schmidt, N. W.; Zhu, R.; Jiang, Y. J.; Lai, G. H.; Wei, G.; Palermo, E. F.; Kuroda, K.; Wong, G. C. L.; Yang, L. H. A Critical Evaluation of Random Copolymer Mimesis of Homogeneous Antimicrobial Peptides. *Macromolecules* **2013**, *46* (5), 1908−1915.
(67) Yang, L. H.; Gordon, V. D.; Trinkle, D. R.; Schmidt, N. W.; Davis, M. A.; DeVries, C.; Som, A.; Cronan, J. E.; Tew, G. N.; Wong, G. C. L. Mechanism of a Prototypical Synthetic Membrane-active Antimicrobial: Efficient Hole-punching via Interaction with Negative Intrinsic Curvature Lipids. *Proc. Natl. Acad. Sci. U. S. A.* **2008**, *105* (52), 20595−20600.
(68) Yang, L.; Gordon, V. D.; Mishra, A.; Som, A.; Purdy, K. R.; Davis, M. A.; Tew, G. N.; Wong, G. C. L. Synthetic Antimicrobial Oligomers Induce a Composition-dependent Topological Transition in Membranes. *J. Am. Chem. Soc.* **2007**, *129* (40), 12141−12147.
(69) Ihre, H.; Hult, A.; Fréchet, J. M. J.; Gitsov, I. Double-Stage Convergent Approach for the Synthesis of Functionalized Dendritic Aliphatic Polyesters Based on 2,2-Bis(hydroxymethyl)propionic Acid. *Macromolecules* **1998**, *31* (13), 4061−4068.
(70) Ponsinet, R.; Chassaing, G.; Vaissermann, J.; Lavielle, S. Diastereoselective Synthesis of β2-Amino Acids. *Eur. J. Org. Chem.* **2000**, *2000* (1), 83−90.

https://dx.doi.org/10.1021/acsami.9b19076
ACS Appl. Mater. Interfaces XXXX, XXX, XXX−XXX